

# Facts and Myths of Dielectric Breakdown Processes—Part I: Statistics, Experimental, and Physical Acceleration Models

Ernest Y. Wu<sup>ID</sup>, *Fellow, IEEE*

**Abstract**—In part I of this article, the current understanding and experimental observations of the so-called first breakdown (BD) phenomena are reviewed and summarized with a focus on BD statistics and voltage/field acceleration models because of their critical importance to reliability projection. Experimental BD data over a wide range of dielectric materials are reviewed together in a common framework. A thorough examination of various analytic BD models with key features is provided in comparison with experimental observations. In addition, we highlight advanced numerical BD models, which bring out more detailed aspects of the BD process. This state-of-the-art review can provide researchers and engineers with a coherent, global understanding to help continue their research work in this exciting field of dielectric BD.

**Index Terms**—Acceleration model, voltage, field, temperature, polarity dependence of breakdown, Poisson area scaling, reliability, statistics, time-dependent dielectric breakdown (TDDB), weakest-link property.

## I. INTRODUCTION

HISTORICALLY, research into dielectric breakdown (BD) or time-dependent dielectric BD (TDDB) as a failure mechanism has focused mainly on SiO<sub>2</sub> dielectrics because of their unique properties as they are suitable for gate insulators in the front-end-of-line (FEOL) applications in the semiconductor industry [1]–[9]. Over the last 30 years, drastic dimension scaling for higher performance has pushed this research field to the forefront due to the diminishing reliability margin that has resulted from dielectric thickness ( $t_{\text{die}}l$ ) reduction [10]. To further enhance the chip performance in advanced nodes, new insulator materials such as high- $\kappa$  stacks (HfO<sub>2</sub>/SiO<sub>2</sub>) and low- $\kappa$  dielectrics (SiOCH) [11] relative to SiO<sub>2</sub>, as well as new spacer materials (SiBCN and SiOCN) [12] relative to Si<sub>3</sub>N<sub>4</sub>, have been introduced or considered in FEOL, back-end-of-line (BEOL), and middle-of-line (MOL) contexts, respectively. For memory applications, BD failure of new insulators, such as MgO, in magnetic random access memory (MRAM) technology, is currently under

Manuscript received April 18, 2019; revised June 27, 2019; accepted July 1, 2019. Date of publication September 18, 2019; date of current version October 29, 2019. The review of this article was arranged by Editor A. Kerber.

The author is with the IBM Research Division, Essex, VT 05452 USA (e-mail: eywu@us.ibm.com).

Color versions of one or more of the figures in this article are available online at <http://ieeexplore.ieee.org>.

Digital Object Identifier 10.1109/TED.2019.2933612

intensive research. Unfortunately, reliability investigations of BD in these different materials and applications have evolved separately for many years, leading to some confusion and misunderstanding lingering in these different research communities. For example, some methodologies originally developed in FEOL gate dielectrics were mischaracterized and/or poorly documented in other areas. Several review articles that cover TDDB reliability issues are available [1]–[9], particularly for FEOL dielectrics. However, a coherent examination of BD phenomena, characterization methodologies, and modeling in various dielectric materials has not emerged yet.

In this article, we bridge these seemingly disconnected topics or areas into a common framework to improve the synergy among different communities so that the readers can have a broad understanding of dielectrics BD in various applications. Moreover, the resistive random access memory (RRAM) community uses the dielectric BD process to create a conducting filament for switching purposes [9]. This common framework that synthesizes disparate research works and results can benefit this new field of RRAM research. After reviewing BD statistics and results such as thickness scaling of scale- and shape- factors in Section II, we provide a more global overview by summarizing experimental observations of BD voltage and temperature characteristics of different dielectrics in Section III. In Section IV, we have focused our discussion on key acceleration models with a summary of their critical features. Finally, several physics-based approaches are discussed including recent advances in the fundamental understanding of dielectric BD using atomistic simulation, followed by a summary in Section V.

## II. BREAKDOWN STATISTICS

Dielectric BD is a stochastic phenomenon requiring a statistical description. The Weibull distribution as a member of the family of extreme-value distributions has been shown to be the most appropriate description of the random nature of dielectric BD in the form of the cumulative density function (CDF) given by

$$F(t) = 1 - \exp[-(t/T_{63})^\beta] \quad (1)$$

where  $t$  is the statistical variable,  $T_{63}$  is the scale factor at 63.2%, and  $\beta$  is the shape factor (also known as the Weibull slope). This CDF is commonly given in the Weibull plot as  $W(t) = \ln(-\ln(1 - F(t)))$  so that  $W(t) = \beta \{\ln(t) - \ln(T_{63})\}$ .

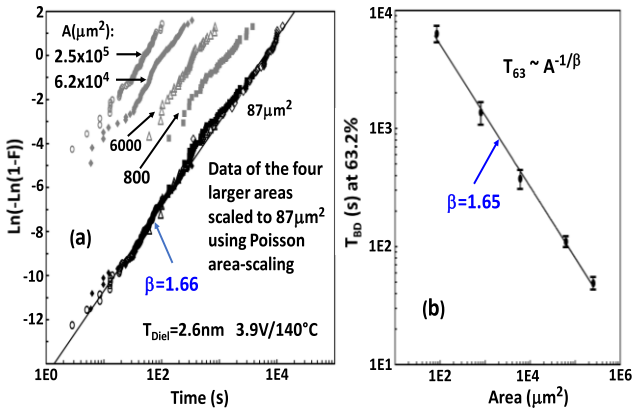


Fig. 1. (a) Normalized  $T_{\text{BD}}$  distributions from the original  $T_{\text{BD}}$  distributions (gray symbols) at different areas for 2.6-nm  $\text{SiO}_2$  by applying Poisson area-scaling. (b)  $T_{\text{BD}}$  at 63% versus area [17].

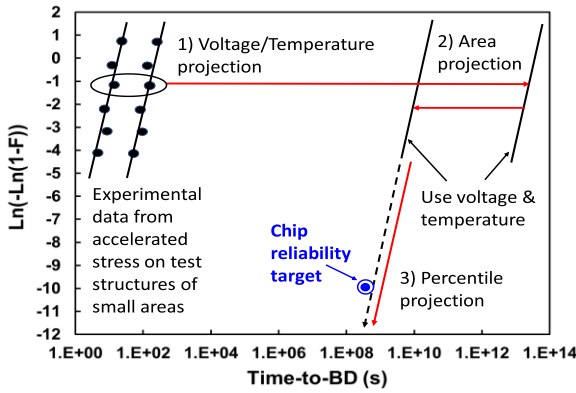


Fig. 2. Reliability projection procedure for dielectric BD as a failure. Three red arrows indicate the key steps in reliability projection.

The Weibull distribution is known to be compatible with the weakest-link property of BD [1]–[5]. This property represents the most fundamental characteristics of BD and can be shown mathematically:  $W_2(t) = W_1(t) + \ln(A_2/A_1)$  for any two areas,  $A_1$  and  $A_2$  (also known as Poisson area scaling). Consequently, the scale factor  $T_{63}$  inversely depends on Area,  $T_{63} \sim A^{-1/\beta}$  as this inverse relation is universally observed over all dielectric materials. Fig. 1(b) shows the  $T_{\text{BD}}$  area-dependence and the fundamental weakest-link property of BD for  $\text{SiO}_2$  gate dielectrics.

Fig. 2 shows the reliability projection procedure from statistical BD data collected at high-stress voltages or temperatures with small devices to low operation voltages or temperatures with a product chip of larger areas. Besides the voltage/temperature extrapolation, as discussed in the next two sections, the important role of Weibull slopes ( $\beta$ ) can be readily seen in the area- and percentile- extrapolation in Fig. 2 [10]. Note for the fixed  $t_{\text{diel}}$ , the use of voltage or field would result in the same projected results.

An important advancement in the field of dielectric BD is the prediction of decreasing  $\beta$  with  $t_{\text{diel}}$  reduction by the percolation model [13]–[15], as shown in Fig. 3, for a wide range of dielectric materials. Based on the concept that BD is triggered as the critical defect density ( $N_{\text{BD}}$ ) is reached [16], the percolation model is capable of connecting  $N_{\text{BD}}$  with a

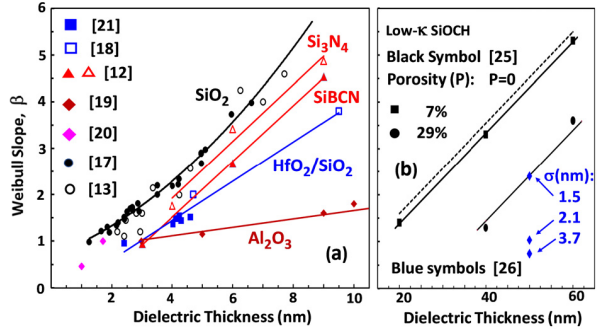
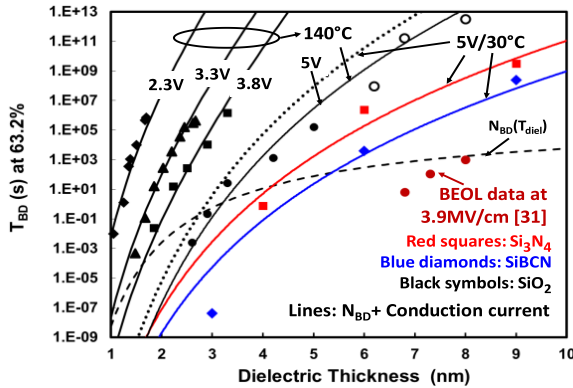


Fig. 3. Thickness dependence of Weibull slopes for  $\text{SiO}_2$  and high- $k$  gate dielectrics as well as (a) MOL spacer materials and (b) BEOL low- $k$  dielectrics. The reduction in the  $\beta$  values due to LER [26] also included for comparison with  $\sigma$  being the LER RMS values.

physical thickness ( $t_{\text{diel}}$ ) [13]–[15]. In comparison with  $\text{SiO}_2$  or MOL dielectrics, high- $k$  stacks ( $\text{HfO}_2/\text{SiO}_2$ ) depict greatly reduced  $\beta$  values (or broader distribution) over a similar thickness range. Some reports attributed the reduced  $\beta$  values of high- $k$  dielectrics to the grain-boundary enhanced defect generation (preexisting or generated) [22]–[24] in competition with other regions. The original percolation model [13]–[15] provides a geometrical description for the filament formation at BD, though the small  $\beta$  values of  $\text{Al}_2\text{O}_3$  were attributed to extrinsic defects [19]. Alternatively, it was recently suggested that the correlation effect may be responsible for these small  $\beta$  values in high- $k$  dielectrics of  $\text{HfO}_2$  and  $\text{Al}_2\text{O}_3$  based on multi-scale atomistic simulation [27]. Some previous reports indicated a change of Weibull slopes depending upon gate electrode materials and ac stress conditions [28]. In contrast to other dielectrics, the  $\beta$  values of low- $k$  BEOL dielectrics (SiOCH) are rather small over a range of much larger  $t_{\text{diel}}$  values [25] with a very large cell-size parameter  $a_0$ . It is shown that porosity [29] and the local field enhancement effects [30] can be responsible for the  $\beta$  reduction. Furthermore, the line-edge roughness (LER) was found to cause a substantial decrease in the measured  $\beta$  values [26] for BEOL low- $k$  dielectrics.

It is important to point out that the shape factors ( $\beta$ ) shown in Fig. 3(a) correspond to the definition of the first BD events, as discussed in Part II. Several reports have shown much higher  $\beta$  values of  $\sim 1.5$  for  $\text{HfO}_2/\text{SiO}_2$  stacks [32], [33]. The percolation model for such dual-layer stacks suggests a non-Weibull distribution with an increased  $\beta$  value at lower percentiles due to the increased  $N_{\text{BD}}$  [34]. Alternatively, this increased  $\beta$  value can be attributed to the progress BD of the second layer after the BD occurrence in the first layer [35].

Despite initial focus on  $\beta$  reduction with  $t_{\text{diel}}$ , it was later realized that  $T_{63}$  reduction with decreasing  $t_{\text{diel}}$  contributes even more shrinkage of the reliability margin [3], [36]. Fig. 4 shows that for thick oxides,  $N_{\text{BD}}$  changes rather slowly but decreases drastically, as  $t_{\text{diel}}$  scales down close to 1 nm [3], [36]. For example, coupling a drastic increase ( $10^{10}$ ) in direct tunneling (DT) current in  $\text{SiO}_2$  with the scaling of  $t_{\text{diel}}$  from 3.5 down to 1.0 nm results in a total  $T_{63}$  reduction of 25 orders of magnitude at the same voltage [3]. These results have significant implications in reliability forecasting and earlier projection in terms of reliability limitation [10], [36]



**Fig. 4.** Thickness dependence of  $T_{BD}$  at 63% for  $\text{SiO}_2$  gate dielectrics [3], MOL spacer materials  $\text{Si}_3\text{N}_4$  and  $\text{SiBCN}$  [12] in comparison with the percolation model. The data of BEOL low- $\kappa$  [31] included for illustration purpose.

for thickness scaling and thus have stimulated considerable research efforts toward the understanding of reliability projection models and their validity. Note that both  $T_{63}$  and  $\beta$  reductions with decreasing  $t_{dielectric}$  are fundamentally correlated, a fact that is often neglected in the literature.

### III. EXPERIMENTAL OBSERVATIONS OF VOLTAGE AND TEMPERATURE DEPENDENCE OF DIELECTRIC BD

In this section, we summarize four  $T_{BD}$  acceleration models frequently discussed in the literature: the exponential law of field/voltage dependence, the exponential law of reciprocal field/voltage dependence, the  $\sqrt{E}$  model, and the power-law voltage/field dependence

$$T_{BD} = T_{BD0} \exp(-\gamma_V V) \sim \exp(-\gamma_E E) \quad (2)$$

$$T_{BD} = T_{BD0} \exp(G_V / V) \sim \exp(G_E / E) \quad (3)$$

$$T_{BD} = T_{BD0} \exp(-\eta_V \sqrt{V}) \sim (-\eta_E \sqrt{E}) \quad (4)$$

$$T_{BD} = ZV^{-m} \sim E^{-m} \quad (5)$$

where  $\gamma_V$ ,  $\gamma_E$ ,  $\eta_V$ ,  $\eta_E$ ,  $G_V$ ,  $G_E$ , and  $m$  represent the voltage or field acceleration factors for these four models. These models are widely used to fit experimental data with an additional parameter, the prefactors,  $T_{BD0}$  or  $Z$  in (2)–(5). The selection of appropriate acceleration models is the most significant in affecting the final projection results of lower-voltages at the use conditions and has been subjected to the intensive debate over many decades. The scaling push for higher transistor performance has led to a drastic  $t_{dielectric}$  reduction and the shrinking of the reliability margin. Moreover, the introduction of low- $\kappa$  dielectrics (SiCOH) in BEOL interconnects [11] and new MOL spacer materials such as SiBCN and SiOCN [12] further raises reliability concerns as the BD properties of these new materials are not well known. While the historical debate 20 years ago between the  $E$ -model [37], [38] and the  $1/E$  model [39], [40] remains academic and unresolved, these debates carry new urgency in engineers' daily qualification work for advanced technology nodes.

A major limitation of dielectric stress for BD study is that the experimental time window usually spans from 1

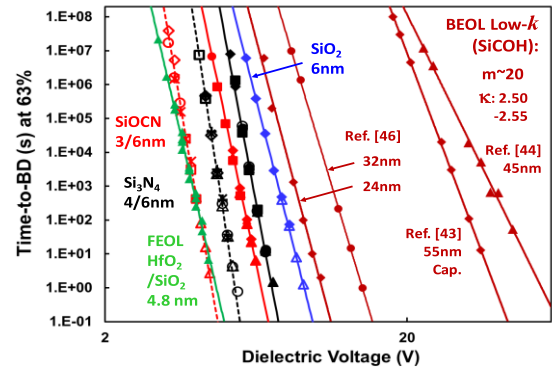


**Fig. 5.**  $T_{BD}$  versus dielectric voltage for several dielectric materials used in FEOL, MOL, and BEOL applications. The BEOL data taken from long-term stress. Note the actual areas and temperature of BEOL data are different whereas for FEOL and MOL data, a fixed area of  $0.5 \mu\text{m}^2$  is used.

to  $\sim 10^4$  s in wafer-level testing. To expand beyond this conventional time-window, several different institutions have carried out long-term stress of up to 3 years at relatively lower stress-voltages. For  $\text{SiO}_2$ , a 3-year stress experiment revealed a  $1/V$  exponential dependence for 6.0-nm [41] oxides whereas another experimental study supports the exponential law dependence (or  $E$  model) for 9.0-nm oxides [42]. In BEOL low- $\kappa$  dielectrics, BD data reported by five institutions for BEOL low- $\kappa$  SiCOH ( $\kappa \sim 2.5$ ) under long-term stress (up to 3 years in [43] and [44]) exhibits the power-law voltage/field dependence [45]–[47]. It is evident that the majority of experimental BD data points to a BD model with a changing voltage/field acceleration factor, rather than a constant acceleration factor as imposed from the exponential law ( $E$ -model). Fig. 5 plots the  $T_{BD}$  versus applied voltage for a variety of materials from BEOL low- $\kappa$ , and MOL spacer dielectrics, to FEOL  $\text{HfO}_2/\text{SiO}_2$  gate dielectrics, showing the power-law voltage/field dependence as the more appropriate acceleration model. The results using SCAPS methodology [48], [49] are also shown in Fig. 5 as an independent experimental demonstration of the power-law model, as discussed below. Finally, note in ultrathick  $\text{SiO}_2$  of 15 nm, it was reported that  $E$  and  $1/E$  models can coexist whereas the  $T_{BD}$  data with the forming-gas anneal in the BEOL process tends to show the  $1/E$  behavior in comparison to  $\text{N}_2$  anneal [50].

Although long-term stress over many years is certainly critical, its throughput is limited because of the long turn-around time. This exercise is clearly impractical for technical qualification and development including evaluation of multiple process recipes and material choices. By the very nature of different possible experimental outcomes, a consensus on a voltage/field acceleration model can emerge if and only if independent experiments can be repeated with similar outcomes. Alternatively, without relying on direct long-term stress, the weakest-link principle (also known as Poisson area-scaling) as the universal dielectric BD property can be used as a criterion to judge a most appropriate acceleration model. This is referred to as the Self-Consistent Acceleration Poisson Statistics (SCAPS) method [48], [49]. This method was first used to demonstrate the power-law voltage dependence as the most reliable description of the acceleration model in  $\text{SiO}_2$

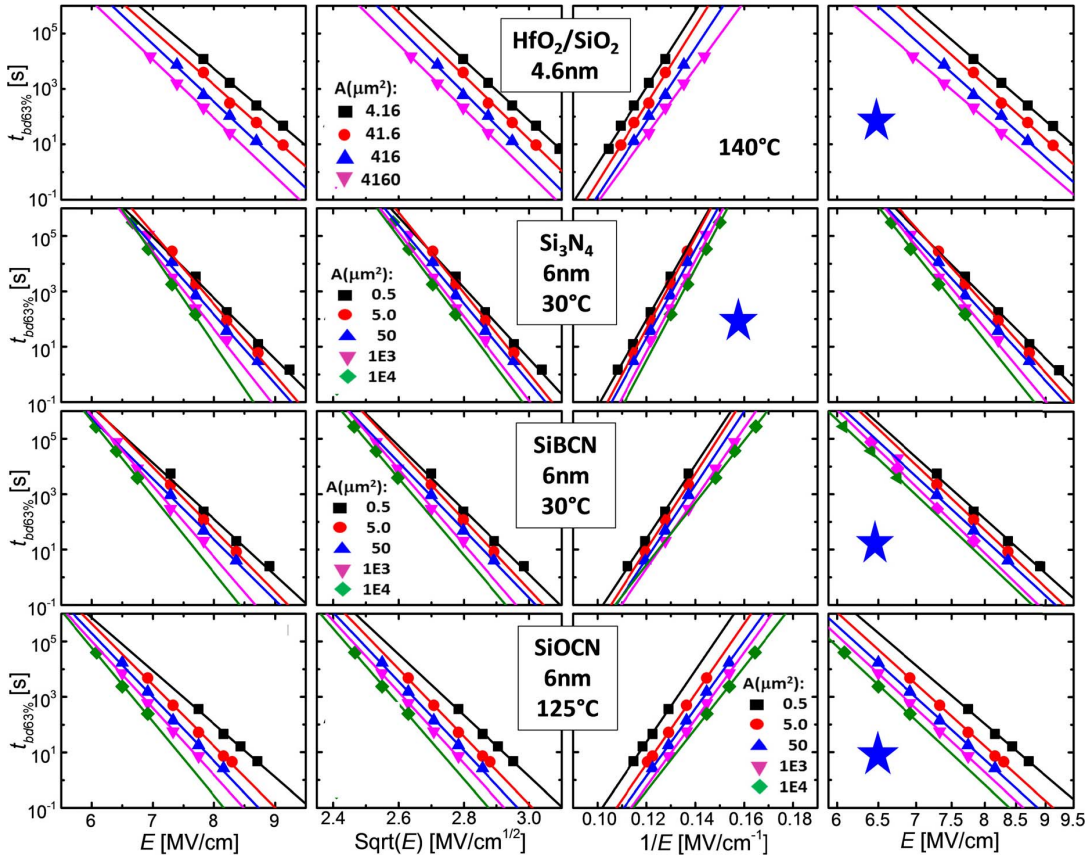


**Fig. 6.**  $T_{BD}$  at 63.2% versus electric fields for several areas are plotted in the four acceleration models [12], [48], [49] (Column 1:  $E$ -model; 2:  $\sqrt{E}$  model; 3:  $1/E$  model; and 4: Power-law model) to examine their compatibility with the weakest-link property of dielectric BD for several dielectric materials. The blue stars indicate the correct acceleration models which preserve the weakest-link property as discussed in the text.

gate dielectrics in the DT regime [48]. The application of this methodology for high- $\kappa$  gate dielectrics [21] and MOL spacer materials [12] is shown in Fig. 6. This figure plots  $T_{BD}$  versus electric fields with several different areas in the form of four different models of (2)–(5). First, the parallel lines from fitting experimental  $T_{BD}$  data indicate that the area-independent acceleration factors are consistent with the weakest-link BD principle. Second, a systematic deviation from the parallel lines means that the extrapolation lines of the  $T_{BD}$  data from different areas would encounter a crossover at lower voltages. This crossover means that  $T_{BD}$  of smaller areas would have been shorter than that of larger areas beyond the crossover point, an unphysical result in the violation of the weakest-link property for a given model. It is interesting to note that while new spacer materials of SiBCN and SiOCN follow the power-law model, the acceleration of  $\text{Si}_3\text{N}_4$  dielectrics is best described by a  $1/E$  model, an observation consistent with a previous publication using pulsed voltage tests and covering ten-orders of time including the memory stress data for Si-rich  $\text{SiN}_x$  [51]. We have also shown previously that BD data for  $\text{SiO}_2$  stressed in Fowler–Nordheim (FN) regime follows a  $1/E$  or  $1/V$  model, but the power-law model can provide a good approximate description for the  $1/E$  model due to the fact that  $1/E$  dependence arises from current field-dependence [49]. Based on these results, we can rule out the  $E$ - and  $\sqrt{E}$ -models as the appropriate acceleration models. Coupling

the long-term stress data with the BD data obtained from the SCAPS method, we can clearly see in Figs. 5 and 6 that the power-law acceleration model is the correct acceleration model for a wide range of materials. It is worthwhile to point out that the application of the SCAPS methodology requires planar structures with well-defined areas. To mimic the realistically integrated structures such as those used in the BEOL applications, planar-structures with capping liners have been carefully designed [52]. Both planar structures and integrated hardware yield comparable  $T_{BD}$  results in support of the power-law model [43], [52].

Because  $T_{BD}$  decreases sharply with decreasing  $t_{dielectric}$ , as shown in Fig. 4, the assessment of  $T_{BD}$  at lower voltages can be made using much thinner dielectrics within a comparable time-window. In this regard, the BD data from  $\text{MgO}$  was collected at voltages as low as 0.9 V and still follows a power-law acceleration model [20], [53]. While using thinner dielectrics, many researchers have adopted pulse tests at much shorter times (down to  $\mu\text{s}$ ) to cover 7–14 decades in time [54]–[58]. The results of using this approach in  $\text{SiO}_2$  ( $1.5 \leq t_{dielectric} \leq 5.0$  nm) [54], [55], BEOL low- $\kappa$  [56], MIMCAP trilayer dielectrics ( $\text{ZrO}_2/\text{Al}_2\text{O}_3/\text{ZrO}_2$ ), and DRAM storage capacitors ( $\text{ZrAl}_x\text{O}_y$ ) [57], [58] indicate a power-law acceleration model. Moreover, the investigation of set-times using a pulse study also yields the power-law dependence over 10 decades in time for RRAM devices [59]. Therefore, a survey of the literature

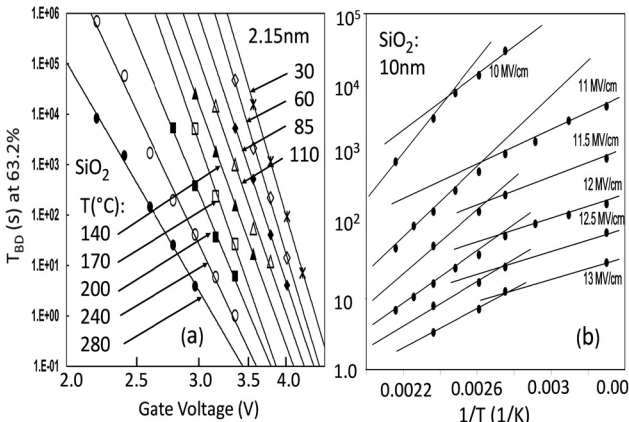


**Fig. 7.** (a) Changing of voltage acceleration factors for various temperatures [70]. (b) Changing of activation energies at different fields (voltages) [63].

results for voltage/field acceleration of dielectric BD over time-spans longer than seven decades (Table I) suggests that the most experimental data consistently points to a universal TDDB power-law acceleration in agreement with the data obtained from long-term stress [41], [43]–[47] and the SCAPS methodology [12], [48], [49] regardless of material types and thickness.

#### A. Temperature and Polarity Dependence

Dielectric BD is not only voltage/field dependent but also temperature-activated. In general, voltage/field acceleration factors are found to decrease with increasing temperature, as shown in Fig. 7(a). In the  $E$ - and  $\sqrt{E}$ -model, the activation energy,  $\Delta H$ , is assumed to be temperature-independent, as in the Arrhenius process [37], [38], [60]–[62]. However, this assumption cannot be supported in many cases. An example of 10-nm  $\text{SiO}_2$  is given in Fig. 7(b), showing that  $\Delta H$  decreases with decreasing temperature and increasing voltage (or field) [63]. Nevertheless, this conventional wisdom of Arrhenius temperature activation has persisted for a long time until  $t_{\text{diel}}$  becomes extremely thin in modern technology nodes in which case this effect becomes more pronounced at lower stress voltages. A new term, the so-called non-Arrhenius activation for  $\text{SiO}_2$  dielectrics, has been used to describe this phenomenon [64]. The Arrhenius temperature dependence tends to be found if the experimental time-window is small with fewer stress voltages or temperatures. The extensive experimental results are reviewed in [3] and [5] as we have discussed this effect in detail along with a discussion of physics-based models in section IV. Another interesting but long-standing debate is the so-called TDDB polarity gap. In this case, the  $T_{\text{BD}}$  data under the nFET accumulation mode with a lower electric field is much shorter than those of the inversion mode with higher electric field [65], as shown in Fig. 8. Note that this gap increases with decreasing  $t_{\text{diel}}$  as the  $T_{\text{BD}}$  ratio of the inversion mode to the accumulation mode approaches  $10^5$ – $10^6$  for thin oxides, as shown in Fig. 8(b).

So far, we have discussed the experimental TDDB results using constant voltage stress (CVS) methodology to directly obtain time-to-BD information. Alternatively, in reliability qualification and/or early process development phases,

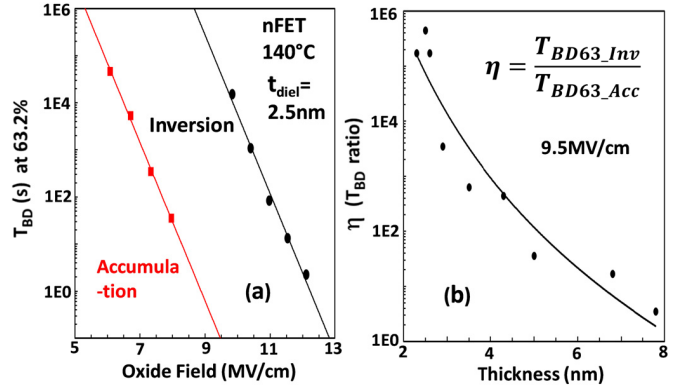


**Fig. 8.** (a)  $T_{\text{BD}}$  versus oxide field for 2.5-nm  $\text{SiO}_2$ . (b)  $T_{\text{BD}}$  ratio ( $\eta$ ) versus  $t_{\text{diel}}$ , showing the polarity gap increases with decreasing  $t_{\text{diel}}$ . The oxide field is obtained by properly correcting surface quantization and poly-depletion effects [66].

ramped-voltage stress (RVS) methodology can be adopted in TDDB assessment. The equivalence and validity of RVS tests have been well-established by the proper transformation of  $V_{\text{BD}}$  (voltage-to-BD) data to  $T_{\text{BD}}$  data, showing excellent agreement with  $T_{\text{BD}}$  data obtained from CVS tests for both FEOL and BEOL dielectrics [67]–[69]. The advantage of the RVS methodology is that it not only reduces the test time but also completes the test in a controlled manner [68]. On the other hand, the ramped voltage stress cannot be used to establish a voltage acceleration model because it is required to convert  $T_{\text{BD}}$  data to  $V_{\text{BD}}$  data as *a priori*.

## IV. PHENOMENOLOGICAL AND/OR PHYSICAL BD MODELS

**Table I** summarizes several phenomenological and/or physics-based BD models reported in the literature for insulating materials ranging from FEOL  $\text{SiO}_2$  gate dielectrics and BEOL low-k  $\text{SiCOH}$  to MOL spacer dielectrics and  $\text{MgO}$  dielectrics. To aid the discussion of each BD model, we will use the following framework (6) to characterize various components influencing the BD process such as current (carrier fluence) and defect generation efficiency (or rate). Based on first-order defect generation kinetics [5], time-to-BD can be derived as

$$T_{\text{BD}} = \frac{q t_{\text{diel}} N_{\text{BD}}(A_{\text{diel}}, t_{\text{diel}})}{J(V, T, t_{\text{diel}}) \xi(V, T, t_{\text{diel}})} \quad (6)$$

with  $q$  being the electron charge.  $J(V, T, t_{\text{diel}})$  is the carrier-conduction current through dielectrics, either by quantum mechanical tunneling or by defect-assisted conduction, which depends on  $t_{\text{diel}}$ , applied voltage ( $V$ ), and temperature ( $T$ ).  $A_{\text{diel}}$  is the dielectric area and  $N_{\text{BD}}$  is the critical defect density at BD [15], which describes statistical BD behaviors such as  $t_{\text{diel}}$ -dependence of  $\beta$  as well as  $T_{\text{BD}}$  area-dependence.  $\xi(V, T, t_{\text{diel}})$  is the defect generation efficiency, also called  $P_{\text{gen}}$  [10], which depends on applied voltage (equivalent to carrier energy) or field and temperature,  $T$ . Using (6), different BD models can be classified into three categories: 1) defect-generation models such as the bond-breakage model or  $E$ -model [37], [38]; 2) carrier-conduction driven models such

TABLE I

SUMMARY OF THE KEY CHARACTERISTICS OF SEVERAL ACCELERATION MODELS FOR DIELECTRIC BD DISCUSSED IN THE TEXT.  
 \*  $L$  IS THE WIRE LENGTH CONSIDERED IN BEOL INTERCONNECTS. \*\* CURRENT CONDUCTION CAN BE INCLUDED EMPIRICALLY [38].  
 \*\*\* FOR COHERENT EXCITATION OF AHR MECHANISM IN  $\text{SiO}_2$ , SEE REFERENCES IN REF. [72], [74]

Key TDDB Models	Const. $\gamma$ E-model [37]	Power-law [3,12, 43–48]	Power-law [49] (as approximation for 1/E model)	1/E model [39,40]	Impact-damage model [77]	$\sqrt{E}$ model [60,61]	$\sqrt{E}$ model w/ Cu diffusion [62]
Mechanism	Thermo-chemical	AHR or Atomistic model	AHR or Atomistic model	Hole generation	Damage creation with PF conduction	Current	Current + Diffusion
Compatibility with percolation	Yes $N_{BD}$	Yes $N_{BD}$	Yes $N_{BD}$	Yes $N_{BD}$	Yes $N_{BD}$	Yes $N_{BD}$	No $N_{BD}^2$
Weakest-link area scaling	Yes	Yes	Yes	Yes	Yes	Yes	Opposite ( $T_{BD} \sim L^2$ ) *
Conduction mechanism	No **	DT	FN (1/E)	FN(1/E)	PF; $\sqrt{E}$	PF; $\sqrt{E}$	Sch; $\sqrt{E}$
Current effect	No	$J^{-1}$ ***	$J^{-1}$	$J^{-1}$	$J^{-1}$	$J^{-1}$	$J^{-2}$
Defect generation rate ( $\xi$ )	Exponential	Power-law	Weak	1/E	1/E	Const	Const
Field or energy driven	Field	Energy and /or Field	Energy and /or Field	Energy and Field	Field	Field	Field
Exp. Demo. w/ $T_{BD} \geq 7$ decades	[42,50]	[12,43–46, 48, 54–59]	[41,49]	[12,41,49, 50,51]	Compatible w/ power-law	?	?
Materials & Applications	$\text{SiO}_2$ , FEOL	$\text{SiO}_2$ , $\text{HfO}_2$ , $\text{SiCOH}$ , $\text{Si}_3\text{N}_4$ , $\text{SiBCN}$ , $\text{ZrO}_2/\text{Al}_x\text{O}_y$ etc; FEOL BEOL, MOL and MIMCaps		$\text{SiO}_2$ , $\text{Si}_3\text{N}_4$	$\text{SiCOH}$	$\text{Si}_3\text{N}_4$	$\text{SiCOH}$

as  $\sqrt{E}$  models [60]–[62]; and 3) fluency-induced defect-generation models such as the anode hydrogen-release model (AHR) [70]–[74], the hole-induced BD models such as the intraband impact ionization 1/E model [39] and anode-hole injection (AHI) model [40], [75], [76], and the impact-damage model [77]. Table I provides a detailed account of individual components, as described in (6) for several BD models. We also provide the experimental verification of these different models in the literature using a criterion ( $T_{BD}$  span  $\geq 7$  decades) for the demonstration time window including the data from the long-term stress tests and SCAPS methodology.

#### A. Field-Drive Versus Energy-Driven Breakdown

Traditionally, the bond-breakage driven by an applied electric field for defects (traps) creation was thought to be the principal or only mechanism for dielectric BD while the role of carrier injection was neglected almost entirely. The original concepts of fluence-driven and energy-driven BD [1] were advanced to examine the correlation between electron energy (gate voltages) at the anode interface and defect generation [78]–[83]. As research has progressed, it has been found that the injected carriers gaining enough energy from electric fields can be responsible for species release [78]–[83] as shown in the framework of AHR and AHI models. Two important pieces of evidence from independent investigations based on the substrate hot electron experiment [79]–[81] and poly-depletion experiment [82] have demonstrated that BD is both fluency-driven and energy (voltage)-driven. The notion

of exclusively field-driven BD is incompatible with the TDDB polarity gap experiment, as mentioned in Section III. Recently, it was suggested that the Lorentz-factor due to the dipole polarization in depletion layers in inversion mode is much smaller than in accumulation mode [84]. Hence, the TDDB polarity gap could have been resolved by plotting the  $T_{BD}$  data against the local field including this so-called Lorentz correction [84]. However, this conclusion is questionable because channel electrons screen out the effect of dipoles in the depletion region. Moreover, the dipole polarizations cannot exclusively affect TDDB while not affecting other electric measurements, such as flat-band voltage, which are shown to be responsible for the dipole effect in high-k/ $\text{SiO}_2$  stacks [85]. In the case of the TDDB polarity gap effect with a conventional poly-Si/ $\text{SiO}_2$ /Si system, the capacitance and flat-bands are well accounted for by full quantum treatment [66] without invoking the dipole effect, as proposed in [84]. As will be discussed in Section IV-D, this polarity gap issue can be resolved entirely by examining the  $Q_{BD}$  data versus the electron energy at the anode [83].

#### B. Constant-Acceleration E-Model

The well-known E-model [37], [38] is based on a thermochemical bond-breakage process due to the lowering of thermal activation energy by the applied field. In this process, the defect generation efficiency is given by  $\xi(E) \sim \exp((\gamma_E E - \Delta H)/k_B T)$ , where  $\Delta H$ ,  $\gamma_E$ ,  $E$ ,  $T$ , and  $k_B$  are the activation energy for Si-O bond breakage, field acceleration

factor, electric field across the dielectric, temperature, and Boltzmann's constant, respectively. This model recently received support from the work of TEM and EELS, which showed that defects (traps) are fundamentally *oxygen vacancies* as a result of BD [9], [86], [87]. Thus, this model provides an important physics-based foundation for the experimental exponential law in (2). However, the constant acceleration factors,  $\gamma_V$  or  $\gamma_E$  derived from (2) are incompatible with the large volume of experimental data as discussed in Section III and also summarized in [5]. However, the thermo-chemical model remains a realistic physical mechanism for the field-induced bond-breakage process. *Thus, we can conclude that the constant-field acceleration E-model is not equivalent to the thermo-chemical model.* Moreover, recent multi-scale atomistic simulation work [88] has reconciled the difference between the thermochemical model and power-law model [89], as discussed in Section IV-E.

### C. Current-Based Model: $\sqrt{E}$ Model

In the BEOL/MOL reliability communities, the  $\sqrt{E}$  model has enjoyed wide acceptance [60]–[62]. Similar to the originally reported findings in FEOL gate dielectrics [1], [78]–[82], correlations between  $T_{BD}$  and conduction currents were also reported and considered in MOL/BEOL dielectrics [60], [61]. Based on these observations, many researchers proposed that the field-acceleration model follows a  $\sqrt{E}$  dependence because electron conduction is believed to be a Poole–Frankel (PF) mechanism. Consequently, these models neglect the field or voltage dependence of defect generation, as outlined in (6).

The PF conduction as a mechanism is widely invoked by many researchers in various reliability and device communities to link it with dielectric degradation and BD. Unlike quantum mechanical tunneling, the foundation of PF conduction is somewhat *ad hoc* as a bulk-limited conduction mechanism [90]. Several recent studies have shed new light on this topic [91]–[93]. First, for a thickness range of 10–100 nm, the contribution of carrier injection (most likely electrons) from the cathode can no longer be ignored [91]. The field dependence of steady-state currents ( $J$ ) can be described by  $\log(J) = a + b\sqrt{E} + \log(1 - c\sqrt{E} - d/E)$  [91]. This electrode-controlled conduction [91] may explain the  $1/E$  dependence of the  $T_{BD}$  data found in thin  $\text{Si}_3\text{N}_4$  films discussed earlier [12], [51]. More importantly, in dielectric materials with large defect density, defect-assisted charge transport takes place through trap-assisted-tunneling (TAT) via electron-phonon coupling and lattice-relaxation [93]. The PF conduction is negligible because the probability of electrons overcoming the barrier by thermal excitation is reduced exponentially with thermal excitation energy [93]. The extracted parameters from the PF conduction are not physically correct [93]. Hence, the use of the PF conduction as a “physics-based” mechanism to justify a BD model is merely a curve-fitting practice using an empirical equation. Moreover, the  $\sqrt{E}$  model is inconsistent with long-term stress data obtained for low- $\kappa$  dielectrics [43]–[47] and the data from SCAPS methodology [12].

One of these  $\sqrt{E}$  models [62] is particularly noteworthy because it was claimed to provide a physics picture for the

Cu-diffusion induced BD process. The model is obtained by manipulating two equations: Schottky conduction with  $\sqrt{E}$  dependence and the Flick diffusion equation. By simply equating diffusion time to  $T_{BD}$ , one obtains a  $\sqrt{E}$  dependence of  $T_{BD}$  [62]. Unlike other BD models, this formulation yields three results in contradiction with the experimental observations: 1)  $T_{BD}$  increases proportionally with increasing wire length ( $T_{BD} \sim L^2$ ) as opposed to the inverse  $T_{BD}$  area dependence ( $T_{BD} \sim A^{-1/\beta}$ ), which arises from the weakest-link principle of the BD process; 2)  $T_{BD}$  is quadratically dependent on  $N_{BD}$  (or Cu concentration at BD) in contradiction with the linear  $N_{BD}$  dependence based on the well-known percolation model [13]–[15]; and 3) it is also shown that Schottky conduction is not a conceivable mechanism for BEOL low- $\kappa$  dielectrics with a large barrier height [94]. These contradictions are direct consequences of equating Cu-diffusion time to  $T_{BD}$  without any justification [62].

### D. Fluency/Energy-Driven Defect Generation Models

**1) Impact Damage Model:  $\sqrt{E} + 1/E$  Model:** Alternatively, it has been proposed that the defect generation rate in BEOL low- $\kappa$  dielectrics [77] is caused by electrons gaining sufficient energy beyond a threshold to create a critical amount of damage at BD. The  $1/E$  dependence is analogous to the mean-free path concept of the impact-ionization rate with a  $1/E$  dependence adopted in the  $1/E$  model for  $\text{SiO}_2$  [39]. Thus, it is called the lucky electron model. While this physics-based model contains three parameters, it is statistically indistinguishable from the power-law (two parameters) in fitting the experimental data [43]. It is interesting to note that the field-dependence of this model is similar to the current conduction form if electrode-controlled tunneling is included [91]. This model has stimulated research efforts in modeling work of BEOL low- $k$  dielectric BD.

**2) Hole-Induced BD and AHI Models:** The so-called  $1/E$  model [39] originally proposed for ultrathick  $\text{SiO}_2$  ( $> 10$  nm) as holes can be generated by incoming electrons within dielectrics via intraband impact ionization (II) [39]. Both the FN current and impact ionization rate for electron-hole pair generation show a  $1/E$  dependence, but the coefficient of FN currents is  $\sim 240$  MV/cm, much larger than that of the II rate ( $\sim 80$  MV/cm) [39]. Thus, the experimental  $T_{BD}$  data showing a  $1/E$  dependence merely reflects the field-dependence of current conduction. Nevertheless, it is still fundamentally a fluence- and energy-driven model, as discussed later. The hole-generation is a well-documented mechanism for the defect generation process, which possibly leads to BD [5], [39], [40], [75], [76], [79]. In ultrathin dielectrics, holes can be injected at anode interfaces via impact-ionization in anodes such as Si, or poly-Si, or metal electrodes [40], [75]. Recently, some authors reconsidered the role of the dominant carrier change (DCC) model based on a kink found in the  $T_{BD}$ -versus- $V_G$  relation for 6.0- and 6.5-nm  $\text{SiO}_2$  [76]. It is unclear why such kinks are only found in such narrow voltage and thickness ranges and not on other  $t_{\text{diel}}$  values [76]. However, it is not prudent to completely exclude the effect of hole-induced defect generation on dielectric BD as it has been widely reported to

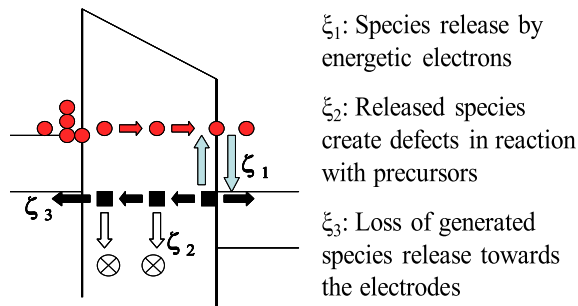


Fig. 9. Schematics for the defect generation processes in species-release process by electrons in the AHR and AHI models.

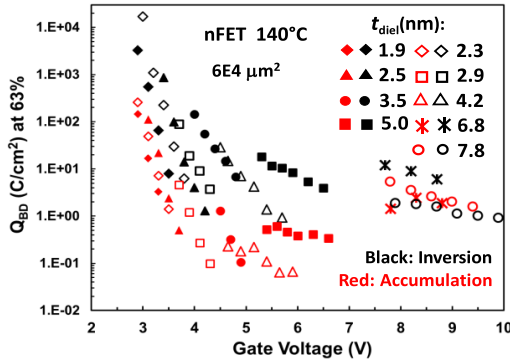


Fig. 10. Polarity-dependent  $Q_{BD}$  versus gate voltage in the absolute value for various thickness values of nFET devices.

be correlated in BD phenomena such as ac TDDB modes and OFF-state TDDB as reviewed in [5] and [95].

**3) Anode Hydrogen-Release Model: Power-Law Model:** In the 1990s, several pioneering experimental studies have focused on hydrogen-release as the key mechanism responsible for dielectric BD [96], [97]. In addition, the first principle calculation has suggested the hydrogen bridge as an electron trap to be responsible for stress-induced leakage current, a forerunner for dielectric BD [98]. In more recent years, the quantitative formulation of the hydrogen-release model has emerged [70]–[74]. Fig. 9 shows a schematic description for species-release induced BD in a two-step process [71]–[73].  $\xi_1$  represents the efficiency of the injected electrons to release hydrogen species at the anode interface,  $\xi_2$  is the probability that released species migrate in the bulk of dielectrics to react with precursors to create defects, and  $\xi_3$  is the probability of released species escaping dielectrics without creating defects. Such a two-step process can be formulated into (6) with  $\xi = \xi_1 k$  and  $k \equiv \xi_2 / (\xi_1 + \xi_2)$  being the reaction process.

To directly extract the defect generation efficiency ( $\xi$ ) from the  $Q_{BD}$  data shown in Fig. 10, we can invert (6) to obtain the following equation [71]:

$$\xi = \frac{q t_{\text{diel}}}{a_0^3 Q_{BD}} \exp \left[ -\frac{1}{\beta(t_{\text{diel}})} \ln \left( \frac{A_{\text{diel}}}{a_0^2} \right) \right]. \quad (7)$$

The single cell-parameter  $a_0$  is independently determined from  $\beta(t_{\text{diel}})$ , as discussed in Section II [15]. The most striking result of this new formulation is that the TDDB polarity gap can be nicely resolved, as shown in Fig. 11(a) and (b). Regardless of stress polarity or device types, the  $Q_{BD}$  voltage-dependence exhibits universal BD characteristics over

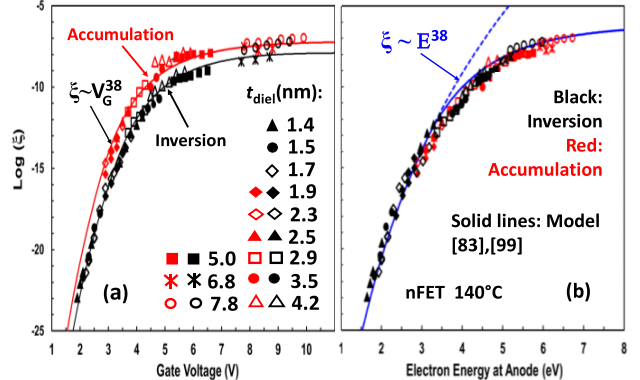


Fig. 11. Defect generation efficiency derived from  $Q_{BD}$  data using a reverse engineering approach [71] with (a) gate voltage and (b) electron energy at the anode as the independent variable. In reference to Fig. 10, additional data of 1.4, 1.5, and 1.7 nm at the lower voltages in the inversion mode are included.

a wide range of  $t_{\text{diel}}$  values. The small gap in the  $Q_{BD}$  versus  $V_G$  plot shown in Fig. 11(a) can be canceled if the maximum electron energy at the anode interface is plotted on the  $x$ -axis rather than the gate voltage [71], [83], [99]. This universal defect generation efficiency reveals a flat region with weak-voltage dependence above 5 V and a sharp decrease with decreasing voltage below 5 V [71]–[73].

By comparing the results shown in Figs. 11(a) or (b) with the H-desorption using scanning tunneling microscopy (STM) [100], one can deduce that above 5 V, a weak  $\xi$  voltage-dependence is due to the electronic excitation (EE) for Si-H breakage [100]. Below 5 V, both coherent excitation [71], [101] and multiple incoherent single vibration excitation [72], [73], [102] can occur with rapid decreasing H-desorption yield. The calculations based on this consideration [71], [72], [99] suggest a unique power-law voltage dependence with a large exponent ( $\sim 38$ ) at 140 °C. Recently, a generalized AHR model including both temperature dependence of the release process ( $\xi_1$ ) due to the thermal occupation of excited vibrational states and thermal activation of the reaction process ( $k$ ) was reported [73]. This provides a good explanation for both the temperature-dependence of exponents and for the non-Arrhenius  $T_{BD}$  temperature activation, as shown in Fig. 12. Some authors have also hypothesized the applicability of the hydrogen-release mode to explain the power-law dependence widely observed in BEOL low- $\kappa$  TDDB data [47]. Despite the successes of the hydrogen-release model, some questions still arise, for example, hydrogen (as foreign-species) induced BD may not represent intrinsic BD of insulators. The H-desorption experiments conducted in a vacuum may not be representative of the  $\text{SiO}_2/\text{Si}$  interface of CMOS devices.

#### E. Numerical Simulation of Dielectric Breakdown

The simple analytic BD models described in Section III are indispensable for engineers working in technical qualification. On the other hand, due to the simplicities of these analytic models, much effort was made to study electron transport and its impact on defect generation as well as on dielectric BD. From the 1980s to the early 1990s, substantial progress was made in the understanding of the interaction of electron-acoustic phonon scattering and the intraband

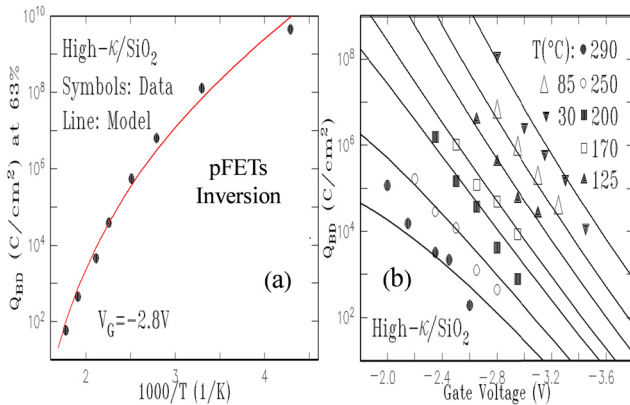


**Fig. 12.** Comparison of the thermally assisted hydrogen release-reaction model [73] (lines) with the  $Q_{BD}$  data (symbols) of high- $\kappa$ /SiO $_2$  bilayers in pFETs stressed under inversion mode. (a) Comparison of non-Arrhenius temperature dependence. (b) Comparison with the  $Q_{BD}$  data at different voltages and temperatures.

impact-ionization (II) process for the electron heating process during transport in thick SiO $_2$  [103]. Based on a four-step kinetic model, the charge-to-BD ( $Q_{BD}$ ) data was related to defect generation due to both trap creation (via hydrogen-release) and electron-hole generation (via II process) over a range of thickness and applied fields [103]. For BEOL low- $\kappa$  dielectrics (SiOCH), the physical model with a set of nonlinear partial differential equations is used to describe the carrier conduction and defect generation [104]. The model qualitatively captures the experimental current transient and a similar field to the  $1/E$  model for dielectric BD in low- $\kappa$  dielectrics. This approach has been extended by including two types of mobile electrons (thermally excited electrons and tunneling electron via traps) for low- $\kappa$  dielectrics [105]. In both approaches, an effective area of  $\sim 0.02\text{--}6\text{ nm}^2$  is required to match the experimental data. This implies an extremely high current density, or an effective trapping efficiency parameter must be invoked to match the data. In addition, the intrinsic statistical aspect of defect generation and its impact on dielectric BD in these modeling approaches were not addressed in contrast with multi-scale atomistic simulation, as we discuss below.

**1) Multi-Scale Atomistic Simulation:** The original  $E$ -model [37] for the Si-O bond breakage is used to link activation energy to its bond strength (4.77 eV or higher) without involving conduction electrons [107]. Under realistic applied electric fields, this bond-strength is too strong to be broken. However, new advances in the numerical calculations using density function theory (DFT) indicate the formation of a new oxygen vacancy with a barrier of  $\sim 0.7$  eV due to the two electrons from carrier injection being trapped in O-Si-O sites [107]. This bond-breakage yields both neutral and negatively charged oxygen vacancies consistent with physical observations [86], [87]. Recently, multi-scale atomistic simulation [88] with the energetic parameters derived from microscopic calculation [107] to predict TDDB statistics and its voltage/field dependence by considering thermochemical Si-O bond breakage and multi-phonon TAT [88], [93]. **Fig. 13(a)** shows the simulation results [88] in excellent agreement with the experimental  $T_{BD}$  distributions of 2.7-nm SiO $_2$  [17]. The calculation results show that the local voltage/field

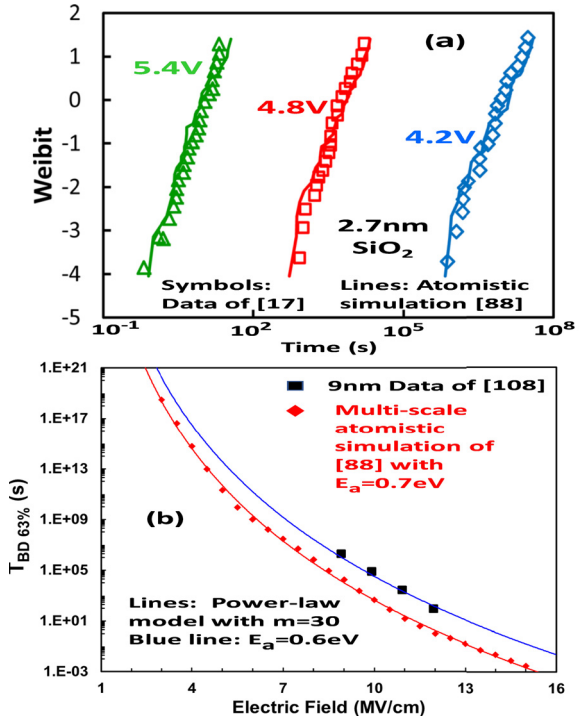


**Fig. 13.** (a) Comparison of multi-scale atomistic modeling results with our  $T_{BD}$  data [17] of 2.7-nm SiO $_2$  stressed in the DT regime. (b) Analysis of [89] showing the simulated  $T_{BD}$  field-dependence [88] as compared to 9-nm data [108], demonstrating the consistency of the power-law model with the results of multi-scale atomistic simulation [88].

acceleration factor increases with decreasing voltage/field, as shown in **Fig. 13(b)**. The further analysis [89] shows that power-law model can well capture the simulation results [88] with its exponent of 30 in agreement with those obtained in the FN regime for thick oxides [41], [49]. These new advances in the microscopic identification of BD defects and atomistic modeling [88], [106], [107] have reconciled the experimental power-law model with the thermochemical model. More importantly, these multi-scale atomistic simulation studies not only accurately describe charge transport through dielectrics but also capture the statistical nature of BD processes including the post-BD phase. Nevertheless, the experimental findings of the TDDB polarity gap and non-Arrhenius temperature dependence remain two unresolved issues from a field-driven approach at this moment.

## V. DISCUSSION AND CONCLUSION

In part 1 of this article, we have attempted a state-of-the-art review of dielectric BD phenomena from a global and coherent viewpoint by covering various applications from FEOL/MOL/BEOL to MRAM/MgO and MIMCAPs with a focus on both experimental observations and physics-based BD models. It is important to judge a voltage/field acceleration model by surveying a large volume of experimental data in the totality with the strong experimental criterion as provided in Table I. In this regard, the BD power-law model or the  $1/E$  model in the FN regime is not merely a set of coincident observations, but rather a general phenomenon based on the universally accepted weakest-link principle. What is often under-appreciated is that accurate experimental data

form the very foundation upon which the physics-based BD models can be developed. The validity of the power-law acceleration model was also demonstrated in comparison with the product HTOL stress at low fields ( $\sim 2$  MV/cm) [46] as will be discussed further in part II.

We have summarized the theoretical efforts that attempt to develop various physics-based BD models by separating *ad hoc* approaches from rigorous theoretical formulations. For example, the popularity and simplicity of PF conduction do not necessarily guarantee its general validity in its relation to dielectric BD processes. In this regard, significant advances made in defect-assisted carrier transport through dielectric materials [93] have clarified the use of the PF conduction equation as merely an empirical fitting procedure. Currently, the majority development efforts of BD model and methodologies among FEOL, BEOL, and MOL communities are mutually exclusive from each other. By applying models and methodologies developed in one community to BD data or issues arising in another, we can verify their validity or limitations and gain deeper insight.

As reviewed in this article, two BD model formulations involving Si-H bond breakage via AHR mechanism or current/field induced Si-O bond breakage via thermo-chemical mechanism (multi-scale atomistic modelling) can provide a good explanation for the power-law acceleration model relevant to  $\text{SiO}_2$  dielectrics. Recently, hydrogen migration induced degradation in the  $\text{SiO}_2/\text{Si}$  system is examined in detail by nuclear reaction analysis, electrical measurements ( $D_{it}$  increase and  $V_{FB}$  shift), and SILC simulation [109]. Similar to the AHI mechanism and also proposed in [36], [38], [75], [76], [79], these authors suggested that hot-holes released by conduction electrons at the anode can back-tunnel and break Si-H bonds at the cathode. Then, the released H atoms during migration generate oxygen vacancies via  $\text{H}_2\text{O}$  desorption based on the first principle calculation [110]. This proposed model seems to explain the polarity gap result and provides a missing piece of the puzzle in the current understanding of dielectric breakdown although many of these hypotheses remain to be verified. In this regard, a species-(by either hydrogen or hole, or both) release model based on the fluency- and energy-driven concept has already provided a good framework to tackle these issues successfully as discussed above. Therefore, introducing species-release mechanisms into multi-scale atomistic simulation is a promising avenue that may eventually unlock the mystery of dielectric breakdown processes. On the other hand, much more work through microscopic modelling and physical identification of BD defects as well as experimental BD measurements are required to further advance our understandings for dielectric materials used in BEOL/MOL, MINCAPS, and MRAM applications.

Regarding the BD acceleration models, a fundamental but rarely discussed issue of dimensionality in the literature, a topic has been discussed recently [111]. A quick examination of model equations from (2) to (5) reveals that the acceleration factor associated with each model carries its signature in its dimensionality (unit) which is fundamentally connected to its mechanism [89], [111]. Because multiple mechanisms are

shown to be responsible for dielectric BD as discussed so far, the power-law acceleration model with a dimensionless exponent provides a more natural description for dielectric BD because a single acceleration factor associated with an individual and specific degradation mechanism is inherently restricted by its dimensionality. In addition, note that a change from voltage (or energy)-driven to a field-driven variable would not fundamentally alter the power-law exponent, an invariant property, which is unique to the power-law acceleration model.

## ACKNOWLEDGMENT

The author would like to thank J. Suñé, J. Stathis, B. Li, E. Nowak, B. Linder, R. Southwick, E. Cartier, R. Muralidhar, T. Ando, A. Kim, G. Bonilla, and V. Narayanan for the long-time collaboration and stimulating discussion. He would also like to thank R. Vollertsen for his kind mentoring when he joined the reliability team and many years of collaborations and his management team, M. Wang, D. Guo, and H. Bu for their constant support.

## REFERENCES

- [1] G. Barbottin and A. Vapaille, *Instabilities in Silicon Devices*. Amsterdam, The Netherlands: Elsevier, 1986, ch. 6, pp. 332–335.
- [2] J. H. Stathis, “Physical and predictive models of ultra thin oxide reliability in CMOS devices and circuits,” in *Proc. IRPS*, Apr./May 2001, pp. 132–149.
- [3] E. Y. Wu and J. Suñé, “Power-law voltage acceleration: A key element for ultra-thin gate oxide reliability,” *Microelectron. Rel.*, vol. 45, pp. 1809–1867, Dec. 2005.
- [4] G. Ribes *et al.*, “Review on high- $k$  dielectrics reliability issues,” *IEEE Trans. Device Mater. Rel.*, vol. 5, no. 1, pp. 5–19, Mar. 2005.
- [5] E. Wu, R. Vollertsen, and J. Suñé, *Reliability Wearout Mechanisms in Advanced CMOS Technologies*, S. Tewksbury and J. Brewer, Eds. Hoboken, NJ, USA: Wiley, 2009, chs. 2–3, pp. 71–329.
- [6] A. Kerber and E. A. Cartier, “Reliability challenges for CMOS technology qualifications with hafnium oxide/titanium nitride gate stacks,” *IEEE Trans. Device Mater. Rel.*, vol. 9, no. 2, pp. 147–162, Jun. 2009.
- [7] R. Degraeve *et al.*, “Review of reliability issues in high- $k$ /metal gate stacks,” in *Proc. 15th Int. Symp. Phys. Failure Anal. Integr. Circuits (IPFA)*, Jul. 2008, pp. 1–6.
- [8] F. Palumbo, C. Wen, S. Lombardo, S. Pazos, F. Aguirre, M. Eizenberg, F. Hui, and M. Lanza, “A review on dielectric breakdown in thin dielectrics: Silicon dioxide, high- $k$ , and layered dielectrics,” *Adv. Func. Mater.*, 2019, Art. no. 1900657.
- [9] J. Suñé, N. Raghavan, and K. L. Pey, *Resistive Switching*, D. Ielmini and R. Waser, Eds. Weinheim, Germany: Wiley, 2016, ch. 8, pp. 225–251.
- [10] J. H. Stathis and D. J. DiMaria, “Reliability projection for ultra-thin oxides at low voltage,” in *IEDM Tech. Dig.*, Dec. 1998, pp. 167–170.
- [11] Z. Tókei, K. Croes, and G. P. Beyer, “Reliability of copper low- $k$  interconnects,” *Microelect. Eng.*, vol. 87, pp. 348–354, Mar. 2010.
- [12] R. G. Southwick, III, E. Wu, S. Mehta, and J. H. Stathis, “Time dependent dielectric breakdown of  $\text{SiN}$ ,  $\text{SiBCN}$  and  $\text{SiOCN}$  spacer dielectrics,” in *Proc. IRPS*, Apr. 2017, pp. DG-1.1–DG-1.5.
- [13] R. Degraeve, G. Groeseneken, R. Bellens, M. Depas, and H. E. Maes, “A consistent model for the thickness dependence of intrinsic breakdown in ultra-thin oxides,” in *IEDM Tech. Dig.*, Dec. 1995, pp. 866–869.
- [14] J. H. Stathis, “Percolation models for gate oxide breakdown,” *J. Appl. Phys.*, vol. 86, no. 10, pp. 5757–5766, Nov. 1999.
- [15] J. Suñé, “New physics-based analytic approach to the thin-oxide breakdown statistics,” *IEEE Electron Device Lett.*, vol. 22, no. 6, pp. 296–298, Jun. 2001.
- [16] J. Suñé, I. Placencia, N. Barniol, E. Farrés, F. Martín, and X. Aymerich, “On the breakdown statistics of very thin  $\text{SiO}_2$  films,” *Thin Solid Films*, vol. 185, pp. 347–362, Mar. 1990.
- [17] E. Y. Wu, J. Suñé, and W. Lai, “On the Weibull shape factor of intrinsic breakdown of dielectric films and its accurate experimental determination. Part II: Experimental results and the effects of stress conditions,” *IEEE Trans. Electron Devices*, vol. 49, no. 12, pp. 2141–2150, Dec. 2002.

- [18] Y. H. Kim *et al.*, "Thickness dependence of Weibull slopes of  $\text{HfO}_2$  gate dielectrics," *IEEE Electron Device Lett.*, vol. 24, no. 1, pp. 40–42, Jan. 2003.
- [19] T. Kauerauf, R. Degraeve, E. Cartier, C. Soens, and G. Groeseneken, "Low Weibull slope of breakdown distributions in high- $k$  layers," *IEEE Electron Device Lett.*, vol. 23, no. 4, pp. 215–217, Apr. 2002.
- [20] S. Van Beek, P. Rousse, B. O'Sullivan, R. Degraeve, S. Cosemans, D. Linten, and G. S. Kar, "Study of breakdown in STT-MRAM using ramped voltage stress and all-in-one maximum likelihood fit," in *Proc. ESSDERC*, Sep. 2018, pp. 146–149.
- [21] E. Wu, "A new formulation of breakdown model for high- $k$ / $\text{SiO}_2$  stack dielectrics," in *Proc. IRPS*, Apr. 2013, pp. 5A.4.1–5A.4.7.
- [22] N. Raghavan, K. L. Pey, K. Shubhakar, and M. Bosman, "Modified percolation model for polycrystalline high- $k$  gate stack with grain boundary defects," *IEEE Electron Device Lett.*, vol. 32, no. 1, pp. 78–80, Jan. 2011.
- [23] M. Masuduzzaman *et al.*, "The origin of broad distribution of breakdown times in polycrystalline thin film dielectrics," *Appl. Phys. Lett.*, vol. 101, Sep. 2012, Art. no. 153511.
- [24] K. S. Yew, D. S. Ang, and G. Bersuker, "Bimodal Weibull distribution of metal/high- $k$  gate stack TDDB—insights by scanning tunneling microscopy," *IEEE Electron Device Lett.*, vol. 33, no. 2, pp. 146–148, Feb. 2012.
- [25] Y. Barbin *et al.*, "Reliability characteristics of thin porous low- $K$  silica-based interconnect dielectrics," in *Proc. IRPS*, Apr. 2013, pp. 2F.3.1–2F.3.5.
- [26] E. Soda, N. Oda, S. Ito, S. Kondo, S. Saito, and S. Samukawa, "Reduction effect of line edge roughness on time-dependent dielectric breakdown lifetime of Cu/low- $k$  interconnects by using CF3I etching," *J. Vac. Sci. Technol. B, Microelectron. Nanometer Struct. Process., Meas., Phenomena*, vol. 27, no. 2, pp. 649–653, 2009.
- [27] A. Padovani and L. Larcher, "Time-dependent dielectric breakdown statistics in  $\text{SiO}_2$  and  $\text{HfO}_2$  dielectrics: Insights from a multi-scale modeling approach," in *Proc. IRPS*, Mar. 2018, pp. 3A.2.1–3A.2.7.
- [28] I. Hirano *et al.*, "Impact of metal gate electrode on Weibull Distribution of TDDB in HfSiON gate dielectrics," in *Proc. IRPS*, Apr. 2009, pp. 355–361.
- [29] E. T. Ogawa, J. Kim, G. S. Haase, H. C. Mogul, and J. W. McPherson, "Leakage, breakdown, and TDDB characteristics of porous low- $k$  silica-based interconnect dielectrics," in *Proc. IRPS*, Mar./Apr. 2003, pp. 166–172.
- [30] S.-C. Lee, A. S. Oates, and K.-M. Chang, "Fundamental understanding of porous low- $k$  dielectric breakdown," in *Proc. IRPS*, Apr. 2009, pp. 481–485.
- [31] Z. Tókei *et al.*, "Role of dielectric and barrier integrity in reliability of sub-100 nm copper low- $k$  interconnects," in *Proc. IRPS*, Apr. 2005, pp. 495–500.
- [32] S. Pae *et al.*, "Gate dielectric TDDB characterizations of advanced high- $K$  and metal-gate CMOS logic transistor technology," in *Proc. IRPS*, Apr. 2012, pp. 5C.1.1–5C.1.5.
- [33] R. Ranjan, T. Nigam, B. Parameshwaran, Y. Liu, and S. F. Yap, "Reliability-performance trade-off for work-function optimization in advanced node replacement metal gate technology," in *Proc. IRPS*, Apr. 2016, pp. DI-8-1–DI-8-5.
- [34] T. Nigam, A. Kerber, and P. Peumans, "Accurate model for time-dependent dielectric breakdown of high- $k$  metal gate stacks," in *Proc. IRPS*, Apr. 2009, pp. 523–530.
- [35] S. Tous, E. Y. Wu, E. Miranda, and J. Suñé, "A strong analogy between the dielectric breakdown of high- $k$  gate stacks and the progressive breakdown of ultrathin oxides," *J. Appl. Phys.*, vol. 109, pp. 1-124115–124115-10, Apr. 2011.
- [36] R. Degraeve, Ed., "Special issue on scaling limits of gate oxides," *Semicond. Sci. Technol.*, 2000, vol. 15, no. 5.
- [37] J. W. McPherson and H. C. Mogul, "Disturbed bonding states in  $\text{SiO}_2$  thin-films and their impact on time-dependent dielectric breakdown," in *Proc. IRPS*, 1998, pp. 47–56.
- [38] J. W. McPherson and R. B. Khamankar, "Molecular model for intrinsic time-dependent dielectric breakdown in  $\text{SiO}_2$  dielectrics and the reliability implications for hyper-thin gate oxide," *Semicond. Sci. Technol.*, vol. 15, no. 5, pp. 462–470, 2000.
- [39] I.-C. Chen, S. E. Holland, and C. Hu, "Electrical breakdown in thin gate and tunneling oxides," *IEEE Trans. Electron Devices*, vol. 32, no. 2, pp. 413–422, Feb. 1985.
- [40] K. F. Schuegraf and C. Hu, "Metal-oxide-semiconductor field-effect-transistor substrate current during Fowler-Nordheim tunneling stress and silicon dioxide reliability," *J. Appl. Phys.*, vol. 76, no. 6, pp. 3695–3700, 1994.
- [41] R.-P. Vollertsen *et al.*, "Long term gate dielectric stress—A timely method?" in *IEDM Tech. Dig.*, Dec. 2006, pp. 1–4.
- [42] J. McPherson, V. Reddy, K. Banerjee, and H. Le, "Comparison of E and 1/E models for  $\text{SiO}_2$  under long-term/low field conditions," in *IEDM Tech. Dig.*, Dec. 1998, pp. 171–174.
- [43] K. Croes, P. Roussel, Y. Barbin, C. Wu, Y. Li, J. Bömmels, and Z. Tókei, "Low field TDDB of BEOL interconnects using >40 months of data," in *Proc. IRPS*, Apr. 2013, pp. 2F.4.1–2F.4.8.
- [44] E. G. Liniger, S. A. Cohen, and G. Bonilla, "Low-field TDDB reliability data to enable accurate lifetime predictions," in *Proc. IRPS*, Jun. 2014, pp. BD.4.1–BD.4.4.
- [45] E. Chery, X. Federspiel, D. Roy, F. Volpi, and J.-M. Chaix, "Identification of the ( $\text{Sq}\sqrt{\text{E}}+1/\text{E}$ )-dependence of porous low- $k$  time-dependent dielectric breakdown using over one year long package levels," *Microelectron. Eng.*, vol. 109, pp. 90–93, Mar. 2013.
- [46] T.-Y. Jeong *et al.*, "Low voltage IMD-TDDB lifetime model for advanced future logic technology nodes," in *Proc. IEEE Int. Interconnect Technol. Conf. (IITC)*, May 2015, pp. 299–302.
- [47] M. N. Chang *et al.*, "A new insight into BEOL TDDB lifetime model for advanced technology scaling," in *IEDM Tech. Dig.*, Dec. 2015, pp. 7.4.1–7.4.4.
- [48] E. Wu *et al.*, "Experimental evidence of TBD power-law for voltage acceleration factors for ultra-thin gate oxide," *IEEE Trans. Electron Devices*, vol. 49, no. 12, pp. 2244–2253, Dec. 2002.
- [49] E. Y. Wu and J. Suñé, "On voltage acceleration models of time to breakdown—Part II: Experimental results and voltage dependence of weibull slope in the FN regime," *IEEE Trans. Electron Devices*, vol. 56, no. 7, pp. 1442–1450, Jul. 2009.
- [50] T. Pompl, K.-H. Allers, R. Schwab, K. Hofmann, and M. Röhner, "Change of acceleration behavior of time-dependent dielectric breakdown by the BEOL process: Indications for hydrogen induced transition in dominant degradation mechanism," in *Proc. IRPS*, Apr. 2005, pp. 388–397.
- [51] R. J. Kaplar, S. D. Habermehl, R. T. Apodaca, B. Havener, and E. Roherty-Osmun, "TDDB and pulse-breakdown studies of Si-rich  $\text{SiN}_x$  antifuses and antifuse-based ROMs," *IEEE Trans. Electron Devices*, vol. 58, no. 1, pp. 224–228, Jan. 2011.
- [52] L. Zhao, Z. Tókei, G. G. Gischia, M. Pantouvaki, K. Croes, and G. Beyer, "A novel test structure to study intrinsic reliability of barrier/low- $K$ ," in *Proc. IRPS*, Apr. 2009, pp. 848–850.
- [53] J. H. Lim *et al.*, "Investigating the statistical-physical nature of  $\text{MgO}$  dielectric breakdown in STT-MRAM at different operating conditions," in *IEDM Tech. Dig.*, Dec. 2018, pp. 25.3.1–25.3.4.
- [54] M. Röhner, A. Kerber, and M. Kerber, "Voltage acceleration of TBD and its correlation to post breakdown conductivity of N- and P-Channel MOSFETs," in *Proc. IRPS*, Mar. 2006, pp. 76–81.
- [55] A. Ille *et al.*, "Ultra-thin gate oxide reliability in the ESD time domain," in *Proc. IEEE Elect. Overstress/Electrostatic Discharge Symp. (EOS/ESD)*, Sep. 2006, pp. 285–294.
- [56] C. LaRow, Z. Chbili, S. F. Yap, A. Kerber, and T. Nigam, "Fast TDDB monitoring for BEOL interconnect dielectrics," in *Proc. IEEE Int. Integr. Rel. Workshop (IIRW)*, Oct. 2017, pp. 1–4.
- [57] J. Y. Seo *et al.*, "Reliability acceleration model of stacked  $\text{ZrO}_2\text{-Al}_2\text{O}_3\text{-ZrO}_2$  MIM capacitor with cylinder type," in *Proc. 26th Int. Conf. Microelectron. (MIEL)*, May 2008, pp. 521–524.
- [58] D. Zhou *et al.*, "Time dependent dielectric breakdown of amorphous  $\text{ZrAl}_x\text{O}_y$  high- $k$  dielectric used in dynamic random access memory metal-insulator-metal capacitor," *J. Appl. Phys.*, vol. 106, pp. 1-044104–104-4, Jul. 2009.
- [59] W.-C. Luo *et al.*, "RRAM SET speed-disturb dilemma and rapid statistical prediction methodology," in *IEDM Tech. Dig.*, Dec. 2012, pp. 215–218.
- [60] K.-H. Allers, "Prediction of dielectric reliability from I-V characteristics: Poole-Frenkel conduction mechanism leading to  $\sqrt{\text{E}}$  model for silicon nitride MIM capacitor," *Microelectron. Rel.*, vol. 44, pp. 411–423, Mar. 2004.
- [61] N. Suzumura *et al.*, "A new TDDB degradation model based on Cu ion drift in Cu interconnect dielectrics," in *Proc. IRPS*, Mar. 2006, pp. 429–484.
- [62] F. Chen *et al.*, "A comprehensive study of low- $k$  SiCH TDDB phenomena and its reliability lifetime model development," in *Proc. IRPS*, Mar. 2006, pp. 46–53.
- [63] R.-P. Vollertsen and W. W. Abadeer, "Upper voltage and temperature limitations of stress conditions for relevant dielectric breakdown projections," *Qual. Rel. Int.*, vol. 11, no. 4, pp. 233–238, 1995.
- [64] D. J. DiMaria and J. H. Stathis, "Non-Arrhenius temperature dependence of reliability in ultrathin silicon dioxide films," *Appl. Phys. Lett.*, vol. 74, no. 12, pp. 1752–1754, Mar. 1999.

- [65] E. Wu *et al.*, "Polarity-dependent oxide breakdown of NFET devices for ultra-thin gate oxide," in *Proc. IRPS*, Apr. 2002, pp. 60–72.
- [66] S.-H. Lo, D. A. Buchanan, and Y. Taur, "Modeling and characterization of quantization, polysilicon depletion, and direct tunneling effects in MOSFETs with ultrathin oxides," *IBM J. Res. Develop.*, vol. 43, no. 3, pp. 327–337, May 1999.
- [67] A. Berman, "Time-zero dielectric reliability test by a ramp method," in *Proc. IRPS*, Apr. 1981, pp. 204–209.
- [68] A. Kerber, L. Pantisano, A. Veloso, G. Groeseneken, and M. Kerber, "Reliability screening of high- $k$  dielectrics based on voltage ramp stress," *Microelectron. Rel.*, vol. 47, pp. 513–517, Apr./May 2007.
- [69] M. Lin and K. C. Su, "Correlation between TDDB and VRDB for low- $k$  dielectrics with square root E model," *IEEE Electron Device Lett.*, vol. 31, no. 5, pp. 494–496, May 2010.
- [70] W. McMahon, A. Haggag, and K. Hess, "Reliability scaling issues for nanoscale devices," *IEEE Trans. Nanotechnol.*, vol. 2, no. 1, pp. 33–38, Mar. 2003.
- [71] J. Suñé and E. Y. Wu, "Hydrogen-release mechanisms in the breakdown of thin SiO<sub>2</sub> films," *Phys. Rev. Lett.*, vol. 92, pp. 1-087601–1-087601-4, Feb. 2004.
- [72] J. Suñé and E. Y. Wu, "Mechanisms of hydrogen release in the breakdown of SiO<sub>2</sub>-based gate oxides," in *IEDM Tech. Dig.*, Dec. 2005, pp. 388–391.
- [73] E. Y. Wu and J. Suñé, "Generalized hydrogen release-reaction model for the breakdown of modern gate dielectrics," *J. Appl. Phys.*, vol. 114, Jun. 2013, Art. no. 014103.
- [74] G. Ribes, S. Bruyere, M. Denais, D. Roy, and G. Ghibaudo, "MVHR (multi-vibrational hydrogen release): Consistency with bias temperature instability and dielectrics breakdown," in *Proc. IRPS*, Apr. 2005, pp. 377–380.
- [75] M. Alam, B. Weir, J. Bude, P. Silverman, and A. Ghetti, "A computational model for oxide breakdown: Theory and experiments," *Microelectron. Eng.*, vol. 59, pp. 137–147, Nov. 2001.
- [76] K. Okada, M. Kamei, and S. Ohno, "Reconsideration of dielectric breakdown mechanism of gate dielectrics on basis of dominant carrier change model," *IEEE Trans. Electron Devices*, vol. 64, no. 11, pp. 4386–4392, Nov. 2017.
- [77] J. R. Lloyd, E. Liniger, and T. M. Shaw, "Simple model for time-dependent dielectric breakdown in inter- and intralevel low- $k$  dielectrics," *J. Appl. Phys.*, vol. 98, pp. 084109-1–084109-6, Sep. 2005.
- [78] D. J. DiMaria, "Explanation for the polarity dependence of breakdown in ultrathin silicon dioxide films," *Appl. Phys. Lett.*, vol. 68, pp. 3004–3006, Mar. 1996.
- [79] R. Degraeve, G. Groeseneken, I. De Wolf, and H. E. Maes, "Oxide and interface degradation and breakdown under medium and high field injection conditions: A correlation study," *Microelect. Eng.*, vol. 28, pp. 313–316, Jun. 1995.
- [80] T. Nigam, "Growth kinetics, electrical characterization and reliability study of sub-5nm gate dielectrics," M.S. thesis, Dept. Elect. Eng., Katholieke Univ. Leuven, Leuven, Belgium, 1999.
- [81] E. M. Vogel, J. S. Suehle, M. D. Edelstein, B. Wang, Y. Chen, and J. B. Bernstein, "Reliability of ultrathin silicon dioxide under combined substrate hot-electron and constant voltage tunneling stress," *IEEE Trans. Electron Devices*, vol. 47, no. 6, pp. 1183–1191, Jun. 2000.
- [82] P. E. Nicollian, W. R. Hunter, and J. C. Hu, "Experimental evidence for voltage driven breakdown models in ultrathin gate oxides," in *Proc. IRPS*, Apr. 2000, pp. 7–15.
- [83] E. Wu and J. Suñé, "New insights in polarity-dependent oxide breakdown for ultrathin gate oxide," *IEEE Electron Device Lett.*, vol. 23, no. 8, pp. 494–496, Aug. 2002.
- [84] J. W. McPherson, "Polarity dependent thermochemical E-model for describing time dependent dielectric breakdown in metal-oxide-semiconductor devices with hyper-thin gate dielectrics," *J. Appl. Phys.*, vol. 120, Aug. 2016, Art. no. 104102.
- [85] K. Kita and A. Toriumi, "Intrinsic origin of electric dipoles formed at high- $k$ /SiO<sub>2</sub> interface," in *IEDM Tech. Dig.*, Dec. 2008, pp. 1–4.
- [86] X. Li, C. H. Tung, K. L. Pey, and V. L. Lo, "The chemistry of gate dielectric breakdown," in *IEDM Tech. Dig.*, Dec. 2008, pp. 1–4.
- [87] K. L. Pey *et al.*, "Physical analysis of breakdown in high- $k$ /metal gate stacks using TEM/EELS and STM for reliability enhancement," *Microelectron. Eng.*, vol. 88, pp. 1365–1372, Jul. 2011.
- [88] A. Padovani, D. Z. Gao, A. L. Shluger, and L. Larcher, "A microscopic mechanism of dielectric breakdown in SiO<sub>2</sub> films: An insight from multi-scale modeling," *J. Appl. Phys.*, vol. 121, pp. 55101-1–55101-10, Mar. 2017.
- [89] E. Wu *et al.*, "Fundamental limitations of existing models and future solutions for dielectric reliability and RRAM applications," in *IEDM Tech. Dig.*, Dec. 2017, pp. 21.5.1–21.5.4.
- [90] J. Frenkel, "On pre-breakdown phenomena in insulators and electronic semi-conductors," *Phys. Rev.*, vol. 54, pp. 647–648, 1938.
- [91] S. Palit and M. A. Alam, "Theory of charging and charge transport in 'intermediate' thickness dielectrics and its implications for characterization and reliability," *J. Appl. Phys.*, vol. 111, Feb. 2012, Art. no. 054112.
- [92] H. Schroeder, "Poole–Frenkel-effect as dominating current mechanism in thin oxide films—An illusion?!" *J. Appl. Phys.*, vol. 117, pp. 215103-1–215103-13, May 2015.
- [93] L. Larcher, A. Padovani, F. M. Puglisi, and P. Pavan, "Extracting atomic defect properties from leakage current temperature dependence," *IEEE Trans. Electron Devices*, vol. 65, no. 12, pp. 5475–5480, Dec. 2018.
- [94] Y. Li, G. Groeseneken, K. Maex, and Z. Tókei, "Real-time investigation of conduction mechanism with bias stress in silica-based intermetal dielectrics," *IEEE Trans. Device Mater. Rel.*, vol. 7, no. 2, pp. 252–258, Jun. 2007.
- [95] D. Varghese, V. Reddy, S. Krishnan, and M. A. Alam, "OFF-state degradation and correlated gate dielectric breakdown in high voltage drain extended transistors: A review," *Microelectron. Rel.*, vol. 54, pp. 1477–1488, Aug. 2014.
- [96] D. J. DiMaria and J. W. Stasiak, "Trap creation in silicon dioxide produced by hot electrons," *J. Appl. Phys.*, vol. 65, no. 6, pp. 2342–2356, Mar. 1989.
- [97] E. Cartier, "Characterization of the hot-electron-induced degradation in thin SiO<sub>2</sub> gate oxides," *Microelectron. Rel.*, vol. 38, pp. 201–211, Feb. 1998.
- [98] P. E. Blöchl and J. H. Stathis, "Hydrogen electrochemistry and stress-induced leakage current in silica," *Phys. Rev. Lett.*, vol. 83, no. 2, pp. 372–375, 1999.
- [99] E. Y. Wu, J. Suñé, and R.-P. Vollertsen, "Comprehensive physics-based breakdown model for reliability assessment of oxides with thickness ranging from 1 nm up to 12 nm," in *Proc. IRPS*, Apr. 2009, pp. 708–717.
- [100] T.-C. Shen *et al.*, "Atomic-scale desorption through electronic and vibrational excitation mechanisms," *Science*, vol. 68, no. 5217, pp. 1590–1592, 1995.
- [101] G. P. Salam, M. Persson, and R. E. Palmer, "Possibility of coherent multiple excitation in atom transfer with a scanning tunneling microscope," *Phys. Rev. B, Condens. Matter*, vol. 49, pp. 10655–10662, Apr. 1994.
- [102] K. Stokbro, B. Y.-K. Hu, C. Thirstrup, and X. C. Xie, "First-principles theory of inelastic currents in a scanning tunneling microscope," *Phys. Rev. B, Condens. Matter*, vol. 58, pp. 8038–8041, Sep. 1998.
- [103] D. Arnold, E. Cartier, and D. J. DiMaria, "Theory of high-field electron transport and impact ionization in silicon dioxide," *Phys. Rev. B, Condens. Matter*, vol. 49, pp. 10278–10297, Apr. 1994.
- [104] G. S. Haase, "A model for electric degradation of interconnect low- $k$  dielectrics in microelectronic integrated circuits," *J. Appl. Phys.*, vol. 105, pp. 1-044908–1-044908-10, Feb. 2009.
- [105] S. P. Ogden, J. Borja, J. L. Plawsky, T.-M. Lu, K. B. Yeap, and W. N. Gill, "Charge transport model to predict intrinsic reliability for dielectric materials," *J. Appl. Phys.*, vol. 118, no. 12, Sep. 2015, Art. no. 124102.
- [106] A. L. Shluger and K. P. McKenna, "Models of oxygen vacancy defects involved in degradation of gate dielectrics," in *Proc. IRPS*, Apr. 2013, pp. 5A.1.1–5A.1.9.
- [107] D. Z. Gao, A.-M. El-Sayed, and A. L. Shluger, "A mechanism for Frenkel defect creation in amorphous SiO<sub>2</sub> facilitated by electron injection," *Nanotechnology*, vol. 27, no. 50, pp. 1-505207–1-505207-7, 2016.
- [108] M. Kimura, "Oxide breakdown mechanism and quantum physical chemistry for time-dependent dielectric breakdown," in *Proc. IRPS*, Apr. 1997, pp. 190–200.
- [109] Y. Higashi *et al.*, "Mechanism of gate dielectric degradation by hydrogen migration from the cathode interface," *Microelectron. Rel.*, vol. 70, pp. 12–21, Mar. 2017.
- [110] K. Kato, "H-H interactions from SiO<sub>2</sub> to SiO<sub>2</sub>/Si(100) interfaces and H-induced O vacancy generation via 3-fold coordinated O in SiO<sub>2</sub>," *J. Appl. Phys.*, vol. 113, pp. 1-133512–1-133512-7, Mar. 2013.
- [111] R. Muralidhar, E. Liniger, T. Shaw, A. Kim, and G. Bonilla, "Towards an appropriate acceleration model for BEOL TDDB," in *Proc. IPRS*, Apr. 2016, pp. DI-5-1–DI-5-6.